International Journal of Nanomedicine

Dovepress
open access to scientific and medical research

Open Access Full Text Article

ORIGINAL RESEARCH

Functional chlorin gold nanorods enable to treat breast cancer by photothermal/photodynamic therapy

This article was published in the following Dove Press journal:
International Journal of Nanomedicine

Lei Liu[1,*]
Hong-Jun Xie[2,*]
Li-Min Mu[1]
Rui Liu[1]
Zhan-Bo Su[1]
Yi-Nuo Cui[1]
Ying Xie[1]
Wan-Liang Lu[1]

[1]Beijing Key Laboratory of Molecular Pharmaceutics and New Drug System, State Key Laboratory of Natural and Biomimetic Drugs, School of Pharmaceutical Sciences, Peking University, Beijing, China; [2]Department of Medicament, College of Medicine, Tibet University, Lhasa, China

*These authors contributed equally to this work

Background: The existing chemo/radiotherapy fail to eliminate cancer cells due to the restriction of either drug resistance or radio tolerance. The predicament urges researchers to continuously explore alternative strategy for achieving a potent curative effect.

Methods: Functional chlorin gold nanorods (Ce6-AuNR@SiO_2-d-CPP) were fabricated aiming at treating breast cancer by photothermal/photodynamic therapy (PTT/PDT). The nanostructure was developed by synthesizing Au nanorods as the photothermal conversion material, and by coating the pegylated mesoporous SiO_2 as the shell for entrapping photosensitizer Ce6 and for linking the D-type cell penetrating peptide (d-CPP). The function of Ce6-AuNR@SiO_2-d-CPP was verified on human breast cancer MCF-7 cells and MCF-7 cells xenografts in nude mice.

Results: Under combinational treatment of PTT and PDT, Ce6-AuNR@SiO_2-d-CPP demonstrated a strong cytotoxicity and apoptosis inducing effects in breast cancer cells in vitro, and a robust treatment efficacy in breast cancer-bearing nude mice. The uptake mechanism involved the energy-consuming caveolin-mediated endocytosis, and Ce6-AuNR@SiO_2-d-CPP in PTT/PDT mode could induce apoptosis by multiple pathways in breast cancer cells.

Conclusion: Ce6-AuNR@SiO_2-d-CPP demonstrated a robust efficacy in the treatment of breast cancer by photothermal/photodynamic therapy. Therefore, the present study could offer a new promising strategy to treat the refractory breast cancer.

Keywords: functional chlorin gold nanorods, cell penetrating peptide, PTT/PDT, cellular uptake, cytotoxicity, apoptosis

Introduction

Breast cancer is the most common cancer among women, and the morbidity worldwide ascended since the 1970s.[1] The conventional therapeutic strategy for breast cancer is a comprehensive treatment by surgery, radiotherapy, chemotherapy, and immunotherapy. Albeit the treatment efficacy for breast cancer had been much improved in evaluation of 5-year survival rate,[2] the existing treatment strategy had no significant effect on the overall survival rate of breast cancer patients. In the disease state, surgical operation is unable to remove all malignant cells, and chemo/radio cannot eliminate the residual cancer cells as well due to the restriction of extensive drug resistance[3,4] and radio tolerance.[5] Moreover, there still lacks an easy accessible immunotherapy to breast cancer patients although the promising chimeric antigen receptor T cell therapy has emerged in the clinical treatment in the latest years.[6] Therefore, this predicament urges scientists to continuously explore alternative strategy for achieving a potent curative effect.

Based on literature report,[7] we further developed a photothermal/photodynamic therapy (PTT/PDT) by constructing the functional chlorin gold nanorods (Ce6-AuNR@

Correspondence: Wan-Liang Lu
Beijing Key Laboratory of Molecular Pharmaceutics and New Drug System, State Key Laboratory of Natural and Biomimetic Drugs, School of Pharmaceutical Sciences, Peking University, 38th Xueyuan Road, Beijing 100191, China
Tel/fax +86 108 280 2683
Email luwl@bjmu.edu.cn

submit your manuscript | www.dovepress.com
Dovepress
http://dx.doi.org/10.2147/IJN.S186974

SiO_2-d-CPP), which enabled to effectively kill breast cancer cells under irradiation of external safe dose of light source. In the nanoconstruct, the gold nanorods (AuNRs) were coated with mesoporous silica, pegylated and modified with D-type cell penetrating peptide (d-CPP), followed by encapsulating chlorin e6 (Ce6). The functional Ce6-AuNR@SiO_2-d-CPP were designed for yielding a photothermal/photodynamic efficacy to kill cancer cells by laser irradiation.

Thermal therapy had been applied to treat cancer but burn injury occasionally occurred due to uncontrolled heating. In the study, we built a PTT for precisely treating cancer tissue without the random burn injury. The approach utilized laser to irradiate photothermal conversion material to generate hyperthermia for killing cancer cells. This fabrication is designed according to the rationale that there is a near infrared laser light bio-window in the range of 750–1,000 nm,[8] and the laser in this range can penetrate body tissue into several centimeters without affecting the normal tissue.[9] For achieving the PTT purpose, AuNRs were then constructed as the photothermal conversion material according to our screening on the performance of photothermal conversion materials.

PDT had been approved by Food and Drug Administration of the United States to treat dermatologic diseases. In the latest years, PDT emerges to be a potential strategy for cancer treatment. In the approach, photosensitizer can be delivered to tumor site, and produce singlet oxygen to kill cancer cells by appropriate laser irradiation. However, to tackle with the vigorous and stubborn growth of cancer cells, a single strategy usually does not work.[10] Therefore, PDT was incorporated into the photothermal treatment by entrapping photosensitizer Ce6 into functional gold nanorods as a photosensitizer. Before encapsulating Ce6, AuNRs were first coated by a mesoporous silica layer, which was used as the carrier of Ce6.

CPPs were a series of oligopeptides, which could facilitate macromolecules penetrating into cells via multiple mechanisms, mainly involving as follows: 1) energy-independent pathways, including inverted micelle model, pore formation model, carpet model, and membrane thinning model; 2) energy-dependent pathway by charge delocalization.[11] Due to their excellent transmembrane transport capability and nonirritant property, CPP-based drug delivery has been explored to treat various diseases, including cancer. However, natural CPPs were constituted by L-type amino acids and easily biodegradable by enzymes in vivo.[12] To avoid the enzyme degradation, retro reversal d-CPP was introduced to replace natural L-type amino acids synthesized by D-type amino acids. Furthermore, d-CPP retains the superior properties of transmembrane transport capability and less immunotoxicity.[13]

Au particles have exhibited good biocompatibility and safety in animals.[14,15] However, uncoated Au particles may be extensively distributed in body tissues by protein adsorption, which would cause less accumulation of Au nanoparticles into tumor tissues.[16] To concentrate AuNRs in tumor tissues after injection, and to enhance uptake by cancer cells, the coating material, mesoporous silica, was pegylated by linking with a functional linking agent, maleimide polyethylene glycol N-hydroxysuccinimide, and conjugating with a retro reversal d-CPP.

The objectives of the present study were to construct the functional Ce6-AuNR@SiO_2-d-CPP aimed at producing a photothermal/photodynamic cure, and to have functional verification in breast cancer cells and breast cancer cell-bearing animals.

Materials and methods

Materials

Chloroauric acid was purchased from Adamas Reagent, Ltd. (Shanghai, China), cetyltrimethylammonium bromide (CTAB) was purchased from Amres Co., Inc. (Radnor, PA, USA), sodium borohydride ($NaBH_4$) was purchased from Acros Organics (Geel, Belgium), silver nitrate ($AgNO_3$) was purchased from Energy Chemical (Shanghai, China), and ascorbic acid (AA) was purchased from Sinopharm Chemical Reagent Co., Ltd. (Shanghai, China). Tetraethoxysilane (TEOS) and (3-aminopropyl) triethoxysilane (APTES) were obtained from Inno-Chem Co., Ltd. (Beijing, China). Maleimide-PEG_{2000}-NHS and $mPEG_{2000}$-NHS were obtained from Ponsure Biotech, Inc. (Shanghai, China), and dCdKdRdRdRdQdRdRdKdKdR, d-CPP was purchased from Apeptide, Inc. (Shanghai, China). Roswell Park Memorial Institute 1640 (RPMI-1640) medium, PBS, penicillin/streptomycin solution, and trypsin–EDTA were purchased form Macgene Co., Ltd. (Beijing, China). FBS was purchased from PAN Biotech GmbH (Aidenbach, Bavaria, Germany). All the other chemicals were commercially available and used without further purification. The deionized water used in the experiments was prepared by Millipore system with a resistivity of 18.2 MΩ·cm.

Human breast cancer MCF-7 cells were obtained from National Infrastructure of Cell Line Resources (Beijing, China). The cells were incubated at 37°C under humidified air containing 5% of CO_2 in RPMI-1640 culture medium

(with 10% FBS), which was supplemented with penicillin/streptomycin.

Synthesis of functional Ce6-AuNR@SiO_2-d-CPP

The synthesis of functional Ce6-AuNR@SiO_2-d-CPP is illustrated in Figure 1, and the procedures are described as the following.

Synthesis of AuNRs

AuNRs were prepared by the conventional seed-mediated growth method.[17,18] Briefly, 600 µL freshly prepared ice-cold 0.01 M $NaBH_4$ was added to the solution containing 8 mL 0.1 M CTAB and 250 µL 0.01 M $HAuCl_4$. After vigorous stirring, the seed suspension was incubated at 30°C for 2 hours. The growth solution contained 1 L 0.1 M CTAB, 25 mL 0.02 M $HAuCl_4$, 10 mL 0.01 M $AgNO_3$, 4 mL 1 M HCl, 6 mL 0.1 M AA. After gently mixing the growth solution, 1.2 mL seed suspension was added dropwise, and the solution was incubated at 30°C overnight to obtain AuNRs. The product was washed with deionized water two times to remove the excess CTAB. Then AuNRs were redispersed in 20 mL of deionized water.

Synthesis of AuNR@SiO_2

The mesoporous silica coating was obtained by the classical Stöber method.[19] Briefly, 0.1 M NaOH was added to adjust the AuNRs suspension pH to 10, then 0.5 mL 20% TEOS/ethanol (v/v) was added thrice dropwise under gentle stirring each at 30-minute intervals. The suspension was incubated at room temperature overnight before adding 0.5 mL 20% APTES/ethanol (v/v), then the suspension was incubated at room temperature overnight again. After incubation, the product was washed several times by ethanol and deionized water. Ion exchange method was utilized to further remove the CTAB. The product was added into 100 mL 10 mg/mL NH_4NO_3 in ethanol, and the suspension was refluxed for 8 hours. Then the product was washed by ethanol and redispersed in deionized water, and the prepared AuNR@SiO_2-NH_2 was stored at 4°C after lyophilization.

Preparation of Ce6-AuNR@SiO_2-d-CPP

An amount of 10 mg AuNR@SiO_2-NH_2 was dispersed in 20 mL PBS (pH 8.0), then 5 mg maleimide-PEG_{2000}-NHS was added into the suspension. The suspension was incubated in ice bath for 2 hours until the reaction finished. Then the intermediate product AuNR@SiO_2-PEG_{2000}-maleimide was washed several times and redispersed in PBS (pH 8.0). The AuNR@SiO_2-$mPEG_{2000}$ was prepared by the same method except using $mPEG_{2000}$-NHS instead of maleimide-PEG_{2000}-NHS.

An amount of 5 mg d-CPP was added into the AuNR@SiO_2-PEG_{2000}-maleimide suspension, and the suspension was incubated in ice bath for 2 hours. Then AuNR@SiO_2-d-CPP was produced, washed, and redispersed in PBS (pH 7.4). A volume of 2 mL 0.5 mg/mL Ce6 was added to 10 mL 0.5 mg/mL AuNR@SiO_2-d-CPP suspension. The suspension was gently stirred for 3 days away from light, then the functional Ce6-AuNR@SiO_2-d-CPP were obtained.

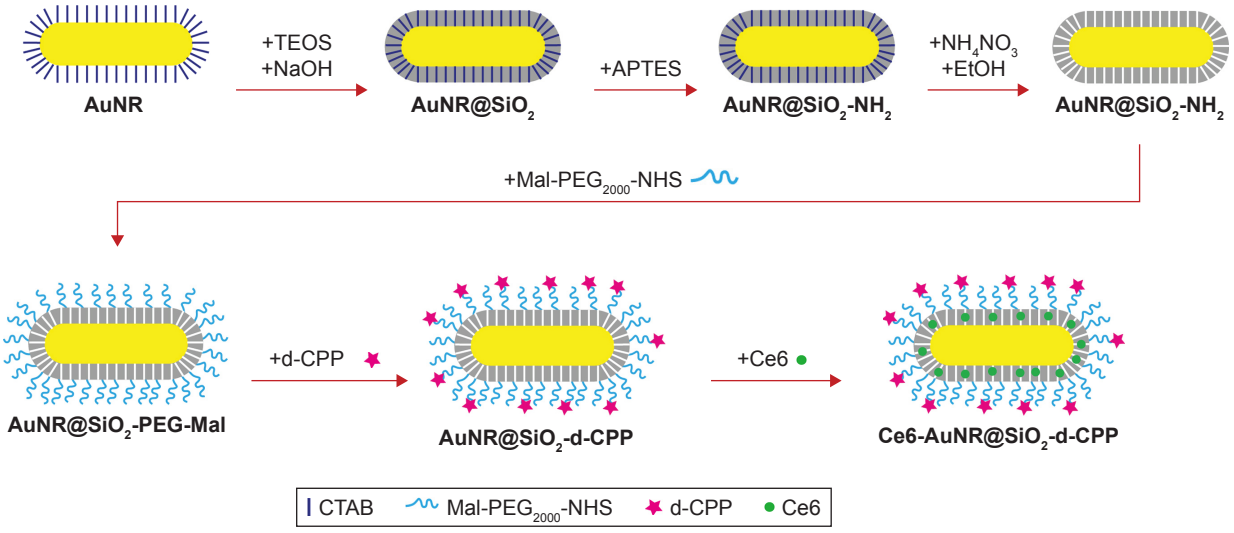

Figure 1 A schematic procedure for preparation of functional chlorin gold nanorods.
Abbreviations: APTES, aminopropyl triethoxysilane; AuNR, Au nanorod; Ce6, chlorin e6; d-CPP, D-type cell penetrating peptide; Mal-PEG2000-NHS, maleimide PEG N-hydroxysuccinimide ester; PEG, polyethylene glycol; TEOS, tetraethyl orthosilicate; CTAB, cetyltrimethylammonium bromide.

Characterization of AuNR@SiO_2-d-CPP

Extinction spectra, potential, size, entrapment, and modifying efficiency

The absorbance spectra of AuNRs were recorded using an ultraviolet–visible–near infrared (UV–Vis–NIR) spectrophotometer (UV-1800PC; Mapada Instruments, Shanghai, China) in the wavelength range of 300–1,000 nm. The zeta potential and the hydrodynamic diameter of AuNR@SiO_2-d-CPP were measured using a Malvern Zetasizer (Malvern Instruments, Malvern, UK). The form of AuNR@SiO_2-d-CPP was observed by JEM1400PLUS transmission electron microscope (JEOL, Tokyo, Japan). The entrapment efficiency of Ce6 was determined by a UV–Vis spectrophotometer at 404 nm. The entrapment efficiency was calculated by the equation: entrapment efficiency = $(W_{\text{Ce6 in Ce6-AuNR@SiO}_2\text{-d-CPP}}/W_{\text{initial weight of Ce6}})\times 100\%$. The amount of d-CPP in Ce6-AuNR@SiO_2-d-CPP was determined by bicinchoninic acid method.[20] The modifying efficiency of d-CPP was calculated by the equation: modifying efficiency = $(W_{\text{d-CPP in Ce6-AuNR@SiO}_2\text{-d-CPP}})/(W_{\text{initial weight of d-CPP}})$.

Ce6 release profiles

To evaluate Ce release in the varying pH values of PBS (without NIR irradiation), 1.0 mL Ce6-AuNR@SiO_2-d-CPP suspension in dialysis tubing was dialyzed against 10 mL varying pH PBS (5.0, 7.4, and 9.0) at 37°C with magnetic stirring. Supernatant 0.5 mL was sampled at specific time points (1, 2, 4, and 8 hours) and centrifuged. After each sampling, an equal volume of PBS was supplemented to the release medium. The released Ce6 in the surfactant was measured by a UV–Vis spectrophotometer at 404 nm. The release rate was calculated by the following equation: release rate = $(C_{\text{Ce6 in PBS}}/C_{\text{initial Ce6}})\times 100\%$.

To evaluate the release of Ce6 from Ce6-AuNR@SiO_2-d-CPP under NIR irradiation, a similar procedure was used but performed under laser light irritation at 808 nm (2 W), each for 6 minutes at 1, 2, 4, and 8 hours.

NIR-induced heating profiles

NIR-induced heating of the AuNRs suspension was performed at 808 nm wavelength laser (Changchun New Industries Optoelectronics Technology Co., Ltd., Changchun, China). AuNRs suspension 1 mL was filled in a well of 24-well plates, and a thermo-sensor was placed in the solution to monitor temperature at 30-second intervals. Then the laser beam was passed through the well from the bottom. The irradiation time was 10 minutes and the temperature was recorded for extra 5 minutes after turning off the laser.

To evaluate the laser power's effect on NIR-induced heating profiles, 1 OD (at 808 nm) AuNRs suspension was filled in 24-well plates, and the laser power was set at 0.5, 1.0, and 1.5 W. To evaluate AuNR concentration's effect on NIR-induced heating profiles, 0.5, 1.0, and 1.5 OD (808 nm) AuNRs suspension was filled in 24-well plates, and the laser power was set at 0.5 W. To evaluate the AuNR's effect on NIR-induced heating profiles, 1 OD (at 808 nm) AuNR, AuNR@SiO_2, or Ce6-AuNR@SiO_2-d-CPP suspension was filled in 24-well plates, and the laser power was set at 1.5 W. NIR-induced heating profiles of PBS were also recorded as the controls.

Cellular uptake by cancer cells and mechanism

To evaluate cellular uptake of AuNR@SiO_2-$mPEG_{2000}$, MCF-7 cells were seeded in 6-well plates at a density of 2×10^6 cells per well and grown in RPMI-1640 medium for 24 hours. The cells were then treated with AuNR@SiO_2-$mPEG_{2000}$, and AuNR@SiO_2-d-CPP in serum-free RPMI-1640 medium at different concentrations (10–40 μg/mL). After treatments, the cellular uptake of AuNRs was measured by a UV–Vis–NIR spectrophotometer.

To evaluate cellular uptake of AuNR@SiO_2-d-CPP, MCF-7 cells were seeded in 35 mm dishes at a density of 2×10^6 cells and incubated in RPMI-1640 medium for 24 hours. The cells were treated with 40 μg/mL AuNR@SiO_2-d-CPP for 6 hours, and then fixed in 2.5% glutaraldehyde. After washing with PBS (pH 7.4), the cells were dehydrated in a graded series of ethanol to prepare the samples. Afterward, the samples were imaged by a transmission electron microscope (JEM1400PLUS; JEOL).

To observe the effect of temperature on the cellular uptake, MCF-7 cells were seeded in 6-well plates at a density of 2×10^6 cells per well and grown in RPMI-1640 medium for 24 hours. The cells were then treated with AuNR@SiO_2-d-CPP in serum-free RPMI-1640 medium at different concentrations (10–40 μg/mL). After 6 hours incubation at 4°C or 37°C, the cellular uptake of AuNRs was measured by a UV–Vis–NIR spectrophotometer.

To reveal the mechanism of cellular uptake, cellular uptake inhibitors for caveolin, clathrin, and micropinocytosis were used.[21] Briefly, MCF-7 cells were seeded in 6-well plates at a density of 2×10^6 cells per well and grown in RPMI-1640 medium for 24 hours. Before treating with AuNR@SiO_2-d-CPP in serum-free RPMI-1640 medium at different concentrations (10–40 μg/mL), the cells were incubated with chlorpromazine (10 μg/mL, 30 minutes), methyl-β-cyclodextrin (10 μM, 30 minutes), and amiloride (50 μM,

1 hour). After 6 hours incubation, the cellular uptake of AuNRs was measured by a UV–Vis–NIR spectrophotometer.

Cytotoxicity by PTT/PDT

To understand the dark cytotoxic effects, MCF-7 cells were seeded in 96-well plates at a density of 6×10^3 cells per well and grown in RPMI-1640 medium for 24 hours. The cells were then treated with Ce6, AuNR@SiO_2-mPEG_{2000}, and Ce6-AuNR@SiO_2-d-CPP in serum-free RPMI-1640 medium at different concentrations (0–100 μg/mL) for 48 hours under dark condition.

To evaluate the PTT cytotoxic effects, MCF-7 cells were cultured as above-mentioned method. The cells were then treated with Ce6, AuNR@SiO_2-mPEG_{2000}, and Ce6-AuNR@SiO_2-d-CPP in serum-free RPMI-1640 medium at different concentrations (0–100 μg/mL) for 12 hours. After replacing the culture media, the wells were irradiated at 808 nm laser (2 W) for 3, 5, and 10 minutes, and then incubated for another 36 hours.

To evaluate the PDT cytotoxic effects, the cell culture and the treatment were performed with the same procedure as that of photothermal evaluation, but the irradiation laser wavelength was set at 650 nm in this experiment.

To evaluate the PTT/PDT cytotoxic effects, MCF-7 cells were cultured and treated with a combination procedure of photothermal and photodynamic evaluations. The irradiation mode was used in the following sequence: 808 nm (2 W) for 10 minutes and 650 nm (50 mW) for 10 minutes.

To observe the live/dead staining images after PTT/PDT treatment, MCF-7 cells were seeded in 24-well plates at a density of 8×10^4 cells per well and incubated in RPMI-1640 medium for 24 hours. The treatment groups consisted of blank control, PDT (free Ce6 with exposure to 50 mW 650 nm laser for 10 minutes), PTT (Ce6-AuNR@SiO_2-d-CPP with exposure to 2 W 808 nm laser for 10 minutes), and PTT/PDT (Ce6-AuNR@SiO_2-d-CPP with exposure to 2 W 808 nm laser for 10 minutes plus 50 mW 650 nm laser for 10 minutes). After treating for 12 hours, the medium was refreshed, and the cells were exposed to laser by aforementioned mode. The cells were further incubated for 12 hours, then stained by calcein AM and ethidium homodimer-1. After 30 minutes incubation, the cells were imaged by a fluorescence microscope (IX-81; Olympus, Tokyo, Japan).

Apoptosis by PTT/PDT and mechanism

To observe the induced apoptosis by PTT/PDT, MCF-7 cells were seeded in 24-well plates at a density of 8×10^5 cells per well and grown in RPMI-1640 medium for 24 hours. The cells were treated with 50 μg/mL Ce6-AuNR@SiO_2-d-CPP for 12 hours in the dark. To exclude the non-uptake nanorods by cancer cells, the culture medium was refreshed. The cells were then treated with PTT (808 nm, 2 W, 5 minutes), PDT (650 nm, 50 mW, 5 minutes), and PTT/PDT mode (808 nm, 2 W, 5 minutes plus 650 nm, 50 mW, 5 minutes). After further 12 hours incubation in the dark, the cells were washed by PBS once, incubated with YO-PRO-1 dye for 30 minutes, and imaged for observing apoptosis by a fluorescence microscope (IX-81; Olympus).

To evaluate the generated singlet oxygen, the experimental samples were prepared as follows: 1) 1 mL 10 mM 1,3-diphenylisobenzofuran (DBPF) solution; 2) 1 mL 10 mM DBPF solution containing free Ce6 (20 μg/mL); 3) 1 mL 10 mM DBPF solution containing Ce6-AuNR@SiO_2-d-CPP (20 μg/mL Ce6); and 4) 1 mL 10 mM DBPF solution containing Ce6-AuNR@SiO_2-d-CPP (20 μg/mL Ce6, followed by 2 W 808 nm laser exposure for 5 minutes to release Ce6 by laser heating). After 50 mW 650 nm laser irradiation for 10–30 seconds, the fluorescence intensity of the experimental samples was recorded by a fluorescence spectrophotometer (Cary Eclipse; Agilent, Santa Clara, CA, USA).

To evaluate the reactive oxygen species (ROS), MCF-7 cells were seeded in 96-well plates at a density of 6×10^3 cells per well and grown in RPMI-1640 medium for 24 hours. The cells were further treated with 50 μg/mL Ce6-AuNR@SiO_2-d-CPP for 12 hours. After refreshing culture medium, the cells were irritated by the same modes as those under "cytotoxicity by PTT/PDT". After laser exposure, the cells were further incubated for 3 hours in the dark. Then the cells were stained by 1 μM 2′,7′-dichlorodihydrofluorescein diacetate for 30 minutes and measured by a multimode reader (FlexStation 3; Molecular Devices, San Jose, CA, USA).

To reveal the mechanism of apoptosis induced by PTT/PDT, MCF-7 cells were seeded in 96-well plates at a density of 6×10^3 cells per well and grown in RPMI-1640 medium for 24 hours. Then the cells were treated with 50 μg/mL Ce6-AuNR@SiO_2-d-CPP for 12 hours. After refreshing culture medium, the cells were irritated by the same modes as those under "cytotoxicity by PTT/PDT". The cells were further incubated for 12 hours in the dark, and then fixed by paraformaldehyde. Afterward, the cells were permeabilized, blocked, and incubated with primary antibodies (anti-caspase 8, anti-caspase 9, and anti-cytochrome C; Sangon, Shanghai, China) or CellEvent Caspase-3/7 Green ReadyProbes Reagent (Thermo Fisher Scientific, Waltham, MA, USA). The primary antibodies were detected after staining with Alexa fluor-488-labeled secondary antibody (Sangon) and Hoechst 33342. The fluorescence intensity

of each well was recorded by the Operetta high-content screening system (PerkinElmer, Waltham, MA, USA).

To observe the mitochondrial membrane potential, MCF-7 cells were seeded in 96-well plates at a density of 6×10^3 cells per well and grown in RPMI-1640 medium for 24 hours. The cells were then treated with 50 μg/mL Ce6-AuNR@SiO_2-d-CPP for 12 hours. After refreshing culture medium, the cells were irritated by the same modes as those under "cytotoxicity by PTT/PDT". The cells were further incubated for 12 hours in the dark. After incubation, the cells were stained with JC-1 for 30 minutes. Then the fluorescence intensity was recorded by a multimode reader (FlexStation 3; Molecular Devices).

In vivo efficacy by PTT/PDT

Female Nu/Nu nude mice were purchased from Beijing Vital River Laboratory Animal Technology Co., Ltd. (Beijing, China). All animal experiments were carried out in accordance with guidelines, and approved by the Committee for Experimental Animal Welfare of Biomedical Ethics of Peking University (LA2016151). The tumor-bearing nude mice models were established by inoculating 2×10^6 MCF-7 cells into the right flanks of the mice. After the tumor volume had reached ~150 mm^3, the mice were randomly divided into four treatment groups (six for each). At day 14, 16, 18, and 20 post inoculation, physiological saline, free Ce6, AuNR@SiO_2-d-CPP, and Ce6-AuNR@SiO_2-d-CPP were given intravenously to mice via tail vein, respectively. The dose was 0.5 mg/kg Ce6 equivalent. The next day after injection, the physiological saline group was not irradiated by light; the Ce6 group was given a 650 nm (50 mW) irradiation for 5 minutes; the AuNR@SiO_2-d-CPP group was given an 808 nm (2 W) irradiation for 5 minutes; and the Ce6-AuNR@SiO_2-d-CPP group was given an 808 nm (2 W) irradiation for 5 minutes plus a 650 nm (50 mW) irradiation for 5 minutes. The laser spot was focused on only the tumor area. The tumor volume and body weight of mice were monitored, and the inhibitory ratio of tumor volume was calculated with following formula: the inhibitory ratio to tumor volume (%) = $V_n/V_{12}\times100$, where V_n is the tumor volume at day n and V_{12} is the tumor volume at day 12. Tumor volume was calculated as length×$width^2/2$ (mm^3).

Statistical analysis

One-way ANOVA was used to determine the significance among groups, after which, post hoc tests with the Bonferroni correction were used for multiple comparisons between individual groups. Data were presented as mean±SD.

Results and discussion

Construction and characterization of Ce6-AuNR@SiO_2-d-CPP

To troubleshoot the potential restriction of chemo/radio therapy, we developed a kind of new functional Ce6-AuNR@SiO_2-d-CPP aimed at eliminating breast cancer cells by PTT/PDT (Figure 1). Such a physicochemical therapy strategy may provide a universal strategy regardless of various subtypes of breast cancer. This is because the approach is a PTT/PDT- based efficacy.

Ce6-AuNR@SiO_2-d-CPP were then constructed in a rod-like Au nanoparticle, which was more suitable for PTT/PDT compared with a sphere-like Au nanoparticle according to our screening (data not shown). To entrap photosensitizer Ce 6, and to reach a better cellular uptake by cancer cells, AuNRs were further coated by mesoporous silicon dioxide, pegylated by PEG containing linking agent, and modified by a D-type of penetrating peptide.

During preparation of AuNRs, the pH values of seed growth media had an impact on the longitudinal plasmon absorbance peak of final products whose wavelengths shifted in the range of 780–820 nm. By adjusting pH value using HCl solution,[22] the maximal absorbance peak of AuNRs was just moved around 800 nm, which was able to fit well with the irradiation wavelength (808 nm) of laser equipment (Figure 2A). Besides, this wavelength was in the scope of the NIR bio-window (750–1,000 nm), which was able to penetrate tissue for several centimeters. This adjustment enabled AuNRs to exert a safe photothermal effect on deep tissue.

AuNRs were uniformly prepared in the shape of oblong rods, and coating shells by SiO_2 or SiO_2-d-CPP were clearly observed (Figure 2B1–B3). The crude AuNR's length, width, and aspect ratio were 52.3±5.2 nm, 14.4±1.5 nm, and 3.6±0.4, respectively. Compared with AuNR, AuNR@SiO_2 had a smooth coating layer of SiO_2 whose thickness was about 20 nm. After PEG/d-CPP modification and Ce6 loading, the surface of Ce6-AuNR@SiO_2-d-CPP turned into rough rod-like surface. In the liquid state, the hydrodynamic diameter of AuNRs increased from 86.3±5.7 nm (AuNR) to 171.0±6.4 nm (Ce6-AuNR@SiO_2-d-CPP) (Table 1). The zeta potential values were 47.3±4.0 mV for AuNR, 28.1±1.7 mV for AuNR@SiO_2, 34.4±1.6 mV for AuNR@SiO_2-d-CPP, and 16.0±0.4 mV for Ce6-AuNR@SiO_2-d-CPP (Figure 2C). After coating and Ce6 loading, the final product of Ce6-AuNR@SiO_2-d-CPP was still positively charged, and the cationic charges of nanoparticles were beneficial for cellular uptake by cancer as the cancer cells were negatively charged. Besides, the decreased positive zeta potential of the final

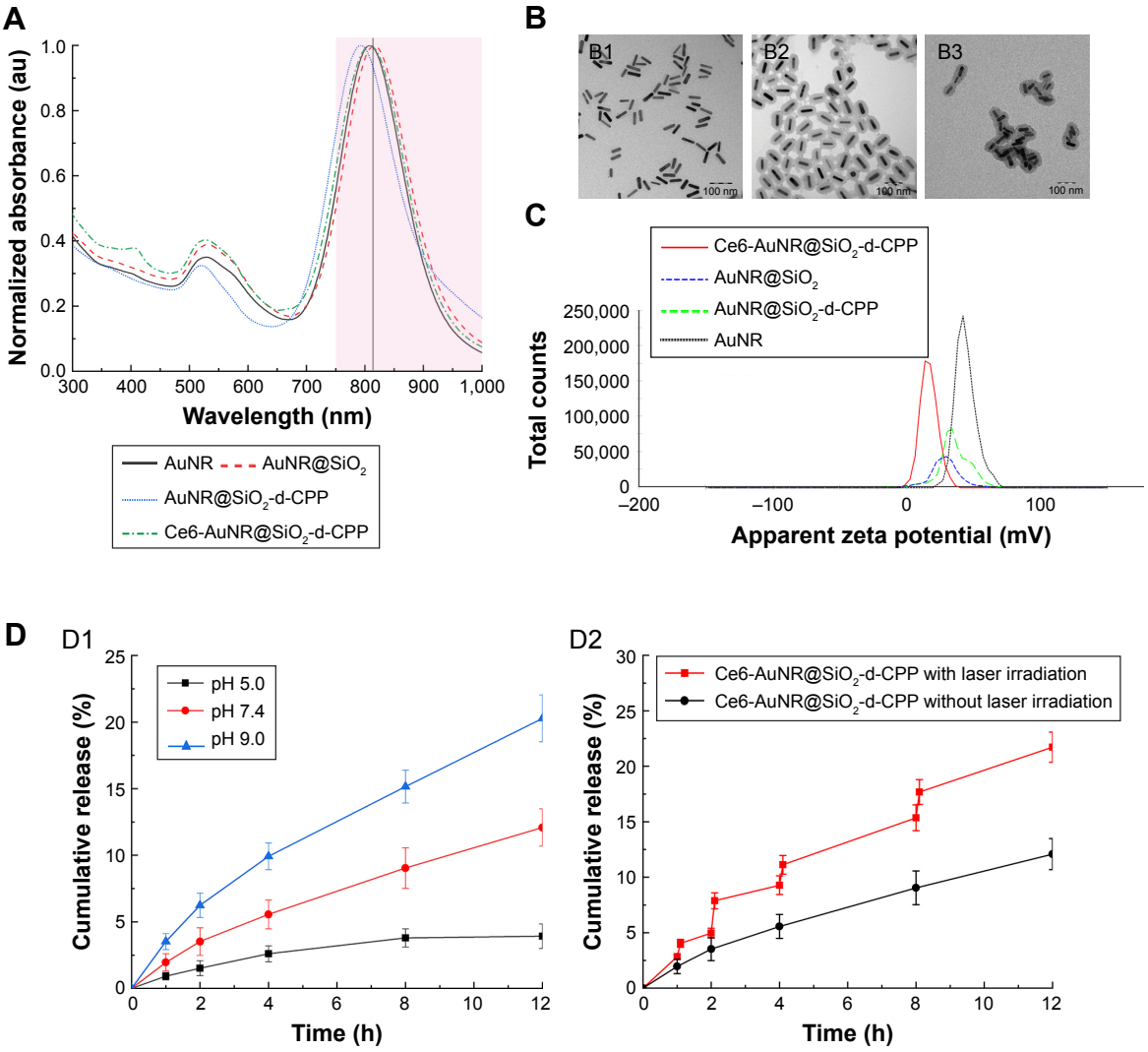

Figure 2 Characterization of functional chlorin gold nanorods.

Notes: (**A**) UV–Vis–NIR spectra of prepared gold nanorods. The vertical line indicates 808 nm and the shaded area represents the near infrared light bio-window. (**B**) TEM image of AuNR (B1), AuNR@SiO$_2$ (B2), and Ce6-AuNR@SiO$_2$-d-CPP (B3). The encapsulation efficiency of Ce6 in Ce6-AuNR@SiO$_2$-d-CPP was 71.2%±1.1% and the modification rate of d-CPP in Ce6-AuNR@SiO$_2$-d-CPP was 23.1%±1.4%. (**C**) Zeta potential distribution of prepared gold nanorods. (**D**) Cumulative Ce6 release rates of Ce6-AuNR@SiO$_2$-d-CPP in the PBS at different pH values (D1), and in the PBS (pH 7.4) after 808 nm NIR exposure (D2). Data are presented as the mean±SD (n=3).

Abbreviations: AuNR, Au nanorod; Ce6, chlorin e6; Ce6-AuNR@SiO$_2$-d-CPP, chlorin gold nanorods; d-CPP, D-type cell penetrating peptide; NIR, near infrared; TEM, transmission electron microscopy; UV–Vis–NIR, ultraviolet–visible–near infrared.

product could also benefit stability of the nanoparticles, and patient tolerance after drug administration due to decreased toxicity. The encapsulation efficiency of Ce6 in Ce6-AuNR@SiO$_2$-d-CPP was 71.2%±1.1% and the modification rate of d-CPP in Ce6-AuNR@SiO$_2$-d-CPP was 23.1%±1.4%.

Table 1 Characterization of gold nanorods

	Size (nm)	Zeta potential (mV)
AuNR	86.3±5.7	47.3±4.0
AuNR@SiO$_2$	93.4±4.9	28.1±1.7
AuNR@SiO$_2$-d-CPP	140.8±10.6	34.4±1.6
Ce6-AuNR@SiO$_2$-d-CPP	171.0±6.4	16.0±0.4

Abbreviations: AuNR, Au nanorod; Ce6, chlorin e6; Ce6-AuNR@SiO$_2$-d-CPP, chlorin gold nanorods; d-CPP, D-type cell penetrating peptide.

The release of Ce6 from Ce6-AuNR@SiO$_2$-d-CPP demonstrated a pH-dependent manner in which the release rate of Ce6 increased with the rising of pH values. At pH 7.4 value nearing a physiological condition, there was only a 12.1%±1.4% release rate at 12 hours, enabling that Ce6 was stable and had a low leaky rate after intravenous administration of Ce6-AuNR@SiO$_2$-d-CPP (Figure 2D1). Furthermore, Ce6 was capable of being released under irradiation of laser (Figure 2D2), showing light-triggering manner, and enabling that, when treating cancer cells, Ce6 was able to be released from the Ce6-AuNR@SiO$_2$-d-CPP to yield PDT effect.

The NIR-induced heating profiles showed a laser power-dependent and AuNR concentration-dependent manners

(Figure S1). Higher laser power or AuNR concentration resulted in a higher temperature due to the heating by irradiation at 808 nm. The results demonstrated that Ce6-AuNR@SiO_2-d-CPP produced significant heating at 808 nm (3°C–14°C rise in temperature) but negligible heating at 650 nm (0.1°C rise in temperature, not shown in Figure S1), suggesting that the irradiation at 650 nm for PDT would not influence the irradiation at 808 nm for PTT (Figure S2), thus avoiding mutual interference of PTT and PDT during the experimental treatment.

Endocytosis by breast cancer cells and mechanism

To exert PDT/PTT cure effect, Ce6-AuNR@SiO_2-d-CPP must be first internalized by cancer cells. The cellular uptake was evidenced by measuring the absorbance of Ce6-AuNR@SiO_2-d-CPP inside breast cancer cells (Figure S3). Compared with control formulation of unmodified Au rods, Ce6-AuNR@SiO_2-d-CPP demonstrated a significant cellular uptake, showing time- and concentration-dependent manners. The study also indicated the action of d-CPP modification that facilitated the AuNRs endocytosis as well.

The cellular uptake by cancer cells of AuNR@SiO_2-d-CPP was clearly observed under transmission electron microscopy in which d-CPP modified nanorods were internalized and formed clusters in endocytic vesicles of breast cancer cells (Figure 3A). To further explain the mechanism of endocytosis, we set up several inhibitor controls, consisting of lower temperature (4°C, Figure 3B), clathrin-mediated endocytosis inhibitor (chlorpromazine, Figure 3C), caveolin-mediated endocytosis inhibitor (methyl-β-cyclodextrin, Figure 3C), and macropinocytosis inhibitor (amiloride, Figure 3C). The results displayed that the lower temperature and methyl-β-cyclodextrin significantly affected the endocytosis of AuNR@SiO_2-d-CPP, indicating that their cellular uptake was endocytosis mediated by multiple factors, involving

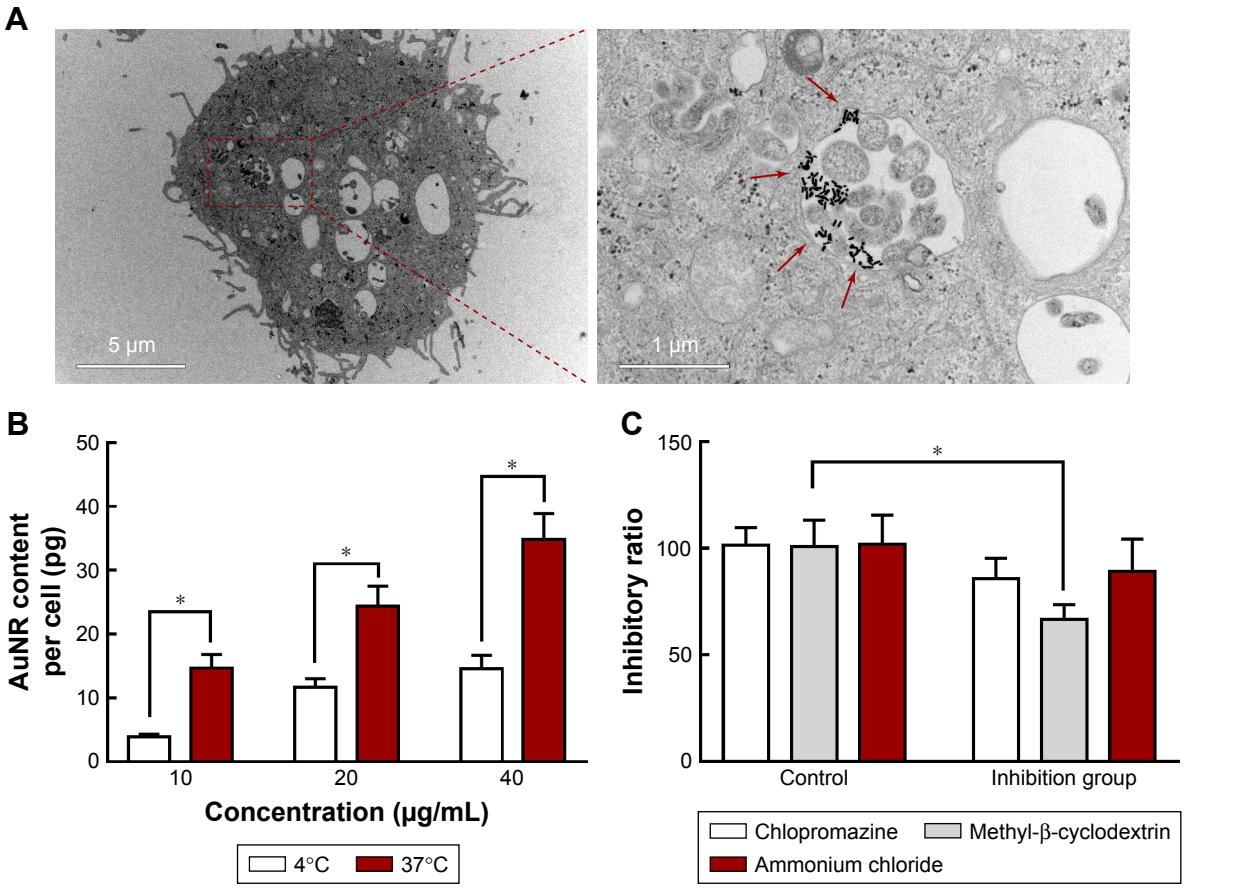

Figure 3 Uptake study of AuNR@SiO_2-d-CPP in the breast cancer cells.
Notes: (**A**) TEM images of AuNR@SiO_2-d-CPP in the breast cancer cells after endocytosis. The right part was the enlarged picture of red dash rectangle in the left part. The arrows indicate AuNR aggregates; (**B**) temperature effect on the uptake by breast cancer cells of AuNR@SiO_2-d-CPP; (**C**) the effects of endocytosis inhibitor on the uptake by breast cancer cells of AuNR. Data are presented as the mean±SD (n=3). *$P<0.05$, vs the controls.
Abbreviations: AuNR, Au nanorod; d-CPP, D-type cell penetrating peptide.

the adenosine triphosphate (ATP) consuming phagocytosis[23] and caveolin-mediated endocytosis.[24] During endocytosis of AuNR@SiO_2-d-CPP, d-CPP played a very important role, by facilitating AuNRs penetration into cancer cells. Albeit the exact mechanism remains unclear, the existing findings suggest that the highly cationic peptide (d-CPP) binds tightly to the anionic lipid membrane, thereby leading to the formation of peptide–lipid salt bridges that permit the translocation across the membrane.[25] Therefore, the d-CPP-modified AuNRs may first bind with the anionic lipid membrane of cancer cells and then transfer across the membrane through the multiple factors' involvement as discussed previously. In this fabrication, an artificially synthesized retro reversal d-CPP was used for significantly retarding the enzyme degradation of naturally occurring L-type CPP.[26,27]

Cytotoxicity of breast cancer cells by PTT/PDT

To evaluate the cytotoxicity of cancer cells by PTT/PDT, Ce6-AuNR@SiO_2-d-CPP formulation was applied to breast cancer cells, and then treated with single or combinational therapeutic modes of both PTT and PDT. 1) First of all, potential cytotoxicity of photosensitizer or AuNRs themselves were precluded under the condition of dark without laser irradiation, and the results showed that the cytotoxicity of free Ce6, AuNR@SiO_2-mPEG, or Ce6-AuNR@SiO_2-d-CPP was negligible in the breast cancer cells (Figure S4A). 2) Furthermore, under the PTT treatment at 808 nm laser irradiation for 3 minutes (Figure S4B1), 5 minutes (Figure S4B2), and 10 minutes (Figure S4B3), free Ce6 had little PTT effect. In contrast, both Ce6-AuNR@SiO_2-d-CPP and AuNR@SiO_2-mPEG exhibited PTT cure effect, and the former showed more potent efficacy (Figure S4B). 3) Besides, under the PDT treatment at 650 nm laser irradiation for 5 minutes (Figure S4C1), 10 minutes (Figure S4C2), and 15 minutes (Figure S4C3), both Ce6-AuNR@SiO_2-d-CPP and AuNR@SiO_2-mPEG had little PDT effect on breast cancer cells while free Ce6 demonstrated a strong PDT effect in a dose-dependent manner (Figure S4C). 4) Finally, under the combinational PTT/PDT treatment at 808 nm irradiation for 10 minutes PTT, and subsequently at 650 nm for 10 minutes PDT, all formulations used exhibited cure effect in the cancer cells, among which, Ce6-AuNR@SiO_2-d-CPP demonstrated the strongest cure effect (Figure S4D).

The aforementioned results indicated that AuNR@SiO_2-mPEG had only PTT effect and free Ce6 had only PDT effect, while Ce6-AuNR@SiO_2-d-CPP had a combinational effect of PTT and PDT. The PTT effect is derived from the heating of AuNR under 808 laser irradiation. It can be explained by the fact that small extent hyperthermia (such as a temperature rise of 5°C) can cause lethal effect in cancer cells through inducing apoptosis and necrosis.[28,29] At the same time, the PDT effect comes from the activation of photosensitizer Ce6. In a specific wavelength, photosensitizer can be inspired by the light to form a singlet state, and further to change into triplet state through electronic spin.[30,31] The activated state of triplet Ce6 can produce ROS by interacting with the surrounding molecules, and the generated ROS caused irreversible damage to cancer cells.[32]

To view the viability of breast cancer cells under therapeutic mode, the live/dead staining intuitively indicated the PTT/PDT effect under fluorescent microscope (Figure 4). The images showed that the live cells were stained in green color by calcein AM while the dead cells were stained in red color by ethidium homodimer-1. Under PDT mode, Ce6-AuNR@SiO_2-d-CPP caused an evident death of cancer cells in viewing the laser boundary. Under PTT mode, Ce6-AuNR@SiO_2-d-CPP resulted in the death of most cancer cells as well. Under combinational PTT/PDT mode, Ce6-AuNR@SiO_2-d-CPP led to the death of nearly all cancer cells. This indicates that the Ce6-AuNR@SiO_2-d-CPP would be a powerful strategy for treating breast cancer, especially by combinational treatment of PTT/PDT.

Apoptosis of breast cancer cells by PTT/PDT and mechanism

To observe the apoptosis induced by PTT/PDT directly, Ce6-AuNR@SiO_2-d-CPP formulation was applied to breast cancer cells, and then treated with a single or combinational treatment of both PTT and PDT. To view the apoptosis directly, the treated breast cancer cells were further stained by Yo-pro-1 fluorescent dye for indicating the apoptotic cells (Figure 5). Similarly, the results demonstrated that Ce6-AuNR@SiO_2-d-CPP caused the strongest apoptosis-inducing effect under the combinational treatment of PTT and PDT compared with the single treatment of either PTT or PDT.

To evaluate the apoptosis induced by PTT/PDT quantitatively, Ce6-AuNR@SiO_2-d-CPP formulation was applied to breast cancer cells, and then treated with a single or combinational treatment of both PTT and PDT. The results from evaluation of singlet oxygen showed that only free Ce6 or the released Ce6 from Ce6-AuNR@SiO_2-d-CPP was able to generate singlet oxygen under laser irradiation at

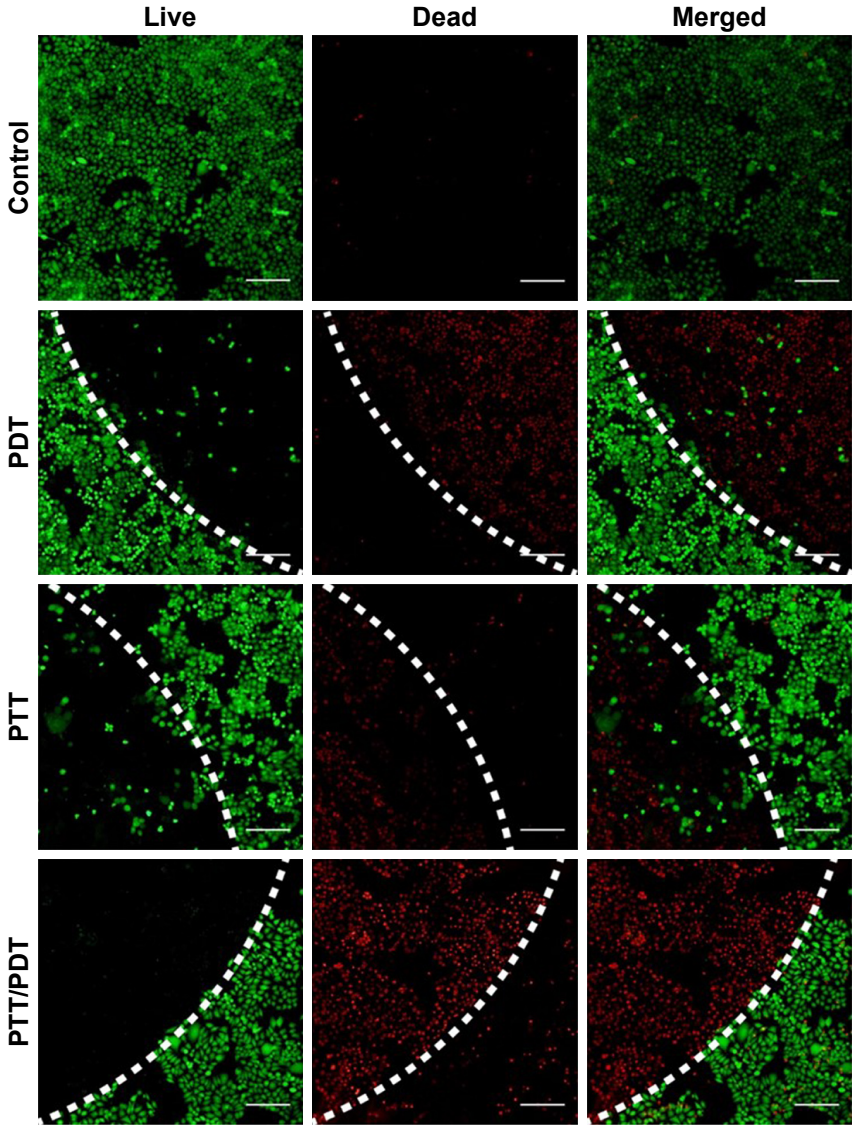

Figure 4 Survival status of breast cancer cells after treatment with Ce6-AuNR@SiO_2-d-CPP under PTT/PDT.
Notes: The survival was observed under fluorescence microscope. The green fluorescence represents live cells stained by calcein AM, while the red fluorescence indicates the dead cells (after laser irradiation) stained by ethidium homodimer. Treatment details: blank control, PDT (free Ce6 with exposure to 50 mW 650 nm laser for 10 minutes), PTT (Ce6-AuNR@SiO_2-d-CPP with exposure to 2 W 808 nm laser for 10 minutes), and PTT/PDT (Ce6-AuNR@SiO_2-d-CPP with exposure to 2 W 808 nm laser for 10 minutes plus 50 mW 650 nm laser for 10 minutes). Scale bar =200 μm.
Abbreviations: AuNR, Au nanorod; Ce6, chlorin e6; Ce6-AuNR@SiO2-d-CPP, chlorin gold nanorods; d-CPP, D-type cell penetrating peptide; PTT/PDT, photothermal/photodynamic therapy.

650 nm (Figure 6A). Furthermore, Ce6-AuNR@SiO_2-d-CPP formulation yielded the strongest ROS (Figure 6B), thereby inducing significant apoptosis.

To further understand the mechanism of apoptosis, the results demonstrated that, under PTT/PDT mode, Ce6-AuNR@SiO_2-d-CPP formulation produced the most significant activations of upstream caspase 8, 9, and downstream caspase 3/7, and the most evidenced release of cytochrome C (Figure 6C), and the most significant decrease in mitochondrial membrane potential (Figure 6D). The apoptotic reactions were induced by Ce6-AuNR@SiO_2-d-CPP under PTT/PDT mode, and the induced apoptosis could be explained by the activations of multiple signaling pathways, involving the activation of death-receptor relevant enzymes (initiator caspase 8 and effector caspase 3/7),[33] the activation of mitochondria-relevant enzymes (initiator caspase 9 and effector caspase 3/7 as well),[34] the opening of mitochondrial permeability transition pore (a decrease of mitochondrial potential and release of cytochrome C),[35] and the ROS generation.[36]

In vivo efficacy by PTT/PDT

To confirm the efficacy, Ce6-AuNR@SiO_2-d-CPP formulation was injected via tail vein into the breast cancer

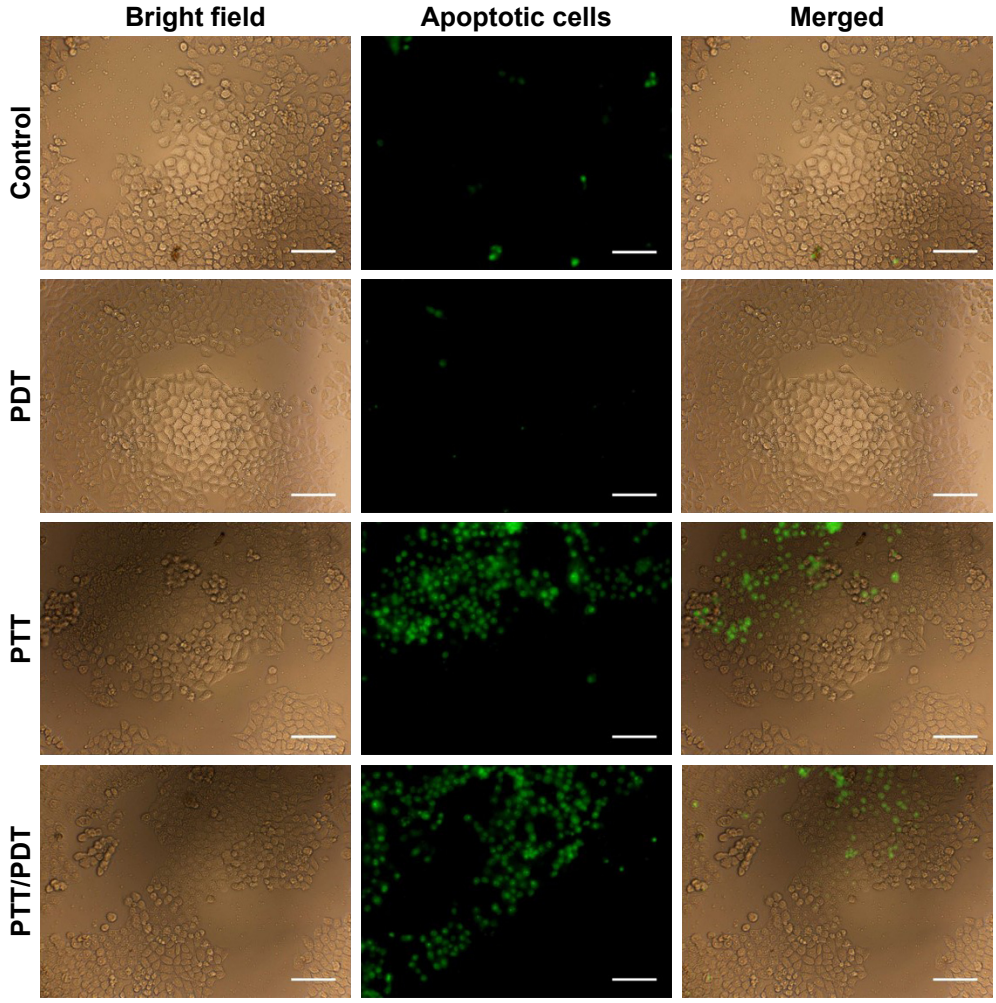

Figure 5 Apoptosis of breast cancer cells after treatment with Ce6-AuNR@SiO_2-d-CPP under PTT/PDT.
Notes: Bright field presents the cell morphology and green channel indicates the early apoptotic cells. The cancer cells were exposed to Ce6-AuNR@SiO_2-d-CPP except control group. Laser irradiation details: blank control (none), PTT (808 nm, 2 W, 5 minutes), PDT (650 nm, 50 mW, 5 minutes), and PTT/PDT (808 nm, 2 W, 5 minutes plus 650 nm, 50 mW, 5 minutes). Scale bar =100 μm.
Abbreviations: AuNR, Au nanorod; Ce6, chlorin e6; Ce6-AuNR@SiO_2-d-CPP, chlorin gold nanorods; d-CPP, D-type cell penetrating peptide; PTT/PDT, photothermal/photodynamic therapy.

xenografts in mice, followed by a combinational treatment of PTT and PDT. The results demonstrated that Ce6-AuNR@SiO_2-d-CPP under PTT/PDT mode exhibited the most powerful anticancer efficacy compared with the control formulations (Figure 7A), and the treatment demonstrated a good safety in viewing preliminary safety evaluation on the body weight change of mice (Figure 7B). Therefore, the animal study was able to verify the functions of both Ce6-AuNR@SiO_2-d-CPP and PTT/PDT treatment mode. After intravenous administration, the significant efficacy in cancer-bearing mice could be associated with the following aspects: long-circulation of the pegylated Ce6-AuNR@SiO_2-d-CPP in blood by evading rapid reticuloendothelial capture;[37] more accumulation of the suitable particle size of nanoparticles into the solid tumor tissues by the enhanced permeability and retention effect;[38] the enhanced cellular uptake of the d-CPP- modified nanoparticles;[39] and the enhanced effect of Ce6-AuNR@SiO_2-d-CPP by PTT and PDT treatment.

Conclusion

We here reported a novel functional Ce6-AuNR@SiO_2-d-CPP, by using AuNRs as the photothermal conversion material, and by coating the pegylated mesoporous SiO_2 as the shell for entrapping photosensitizer Ce6 and for linking the d-CPP. Under combinational treatment of PTT and PDT, Ce6-AuNR@SiO_2-d-CPP demonstrated a strong cytotoxicity and apoptosis-inducing effects in breast cancer cells in vitro, and a robust treatment efficacy in breast cancer-bearing mice. The study further revealed the action mechanisms of cellular uptake and apoptosis in breast cancer cells. In conclusion, the functional Ce6-AuNR@SiO_2-d-CPP could be effectively used

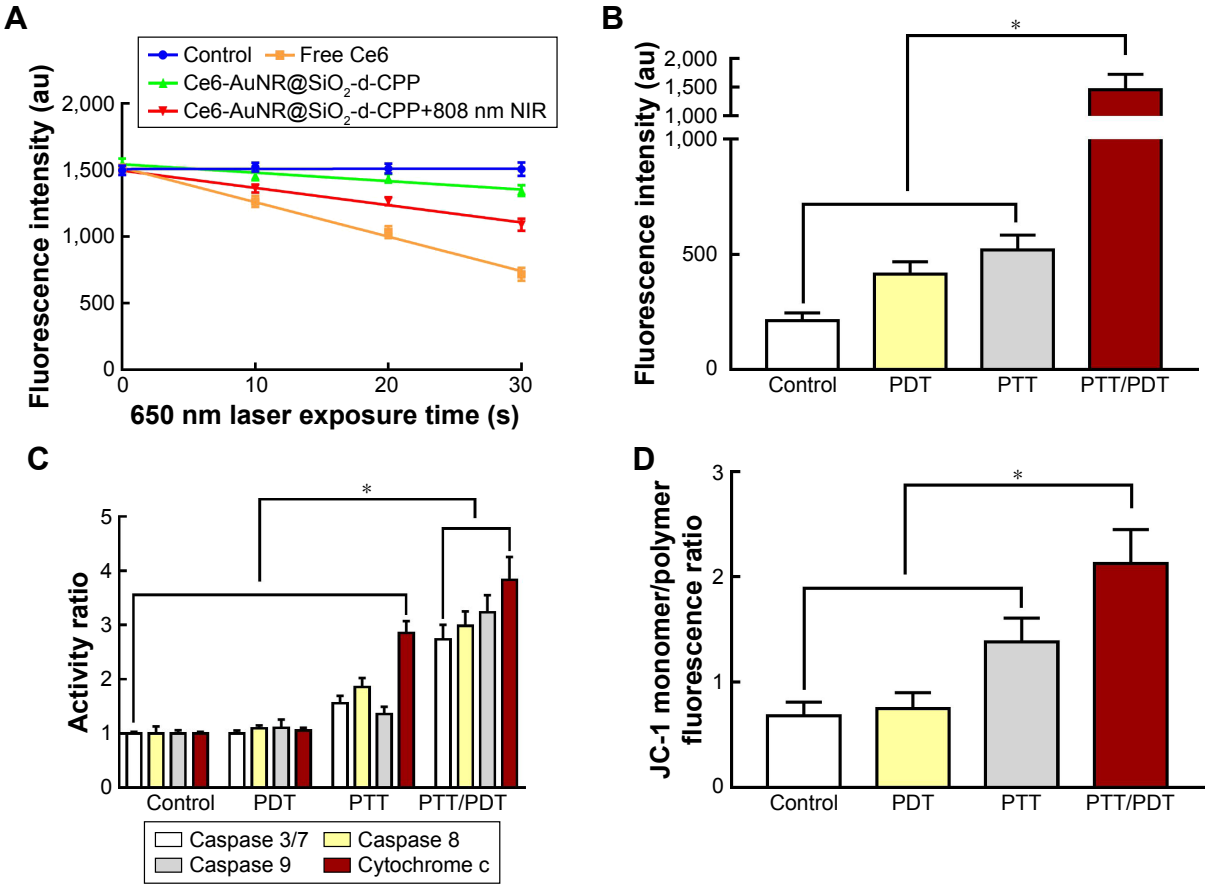

Figure 6 Apoptotic mechanism of breast cancer cells after treatment with Ce6-AuNR@SiO_2-d-CPP under PTT/PDT.

Notes: (**A**) The produced singlet oxygen levels in liquid state under different laser irradiation modes measured by a fluorescence spectrophotometer; (**B**) the ROS levels in breast cancer cells after treatment with Ce6-AuNR@SiO_2-d-CPP under PTT/PDT laser irradiations recorded by a multimode reader; (**C**) activity ratios of upstream apoptotic enzymes caspase 8, 9, downstream caspase 3/7, and apoptotic protein cytochrome C measured by the Operetta high-content screening system; (**D**) the changes of mitochondrial membrane potential recorded by a multimode reader. Data are presented as the mean±SD (n=3). *$P<0.05$, vs the controls.

Abbreviations: AuNR, Au nanorod; Ce6, chlorin e6; Ce6-AuNR@SiO_2-d-CPP, chlorin gold nanorods; d-CPP, D-type cell penetrating peptide; PTT/PDT, photothermal/photodynamic therapy; ROS, reactive oxygen species.

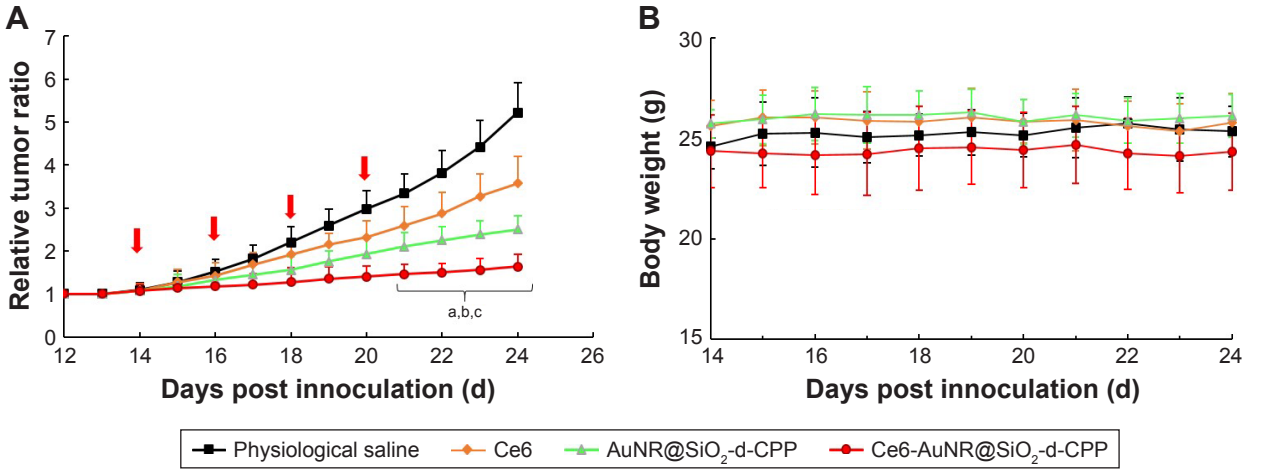

Figure 7 Anticancer efficacy in breast cancer xenografts in nude mice after treatment with Ce6-AuNR@SiO_2-d-CPP under PTT/PDT.

Notes: This figure depicts the relative tumor ratio (**A**) and body weight (**B**) of tumor-bearing nude mice after treatment with functional chlorin gold nanorods under photothermal/photodynamic treatment mode. Ce6-AuNR@SiO_2-d-CPP was intravenously injected into breast cancer tumor-bearing mice via tail vein at day 14, 16, 18, and 20 post inoculation. After treatment under PTT/PDT, the anticancer efficacy was estimated by the tumor volume ratio. The experiment groups consisted of physiological saline group (without irradiation), free Ce6 group (PDT by 650 nm 50 mW laser irradiation for 5 minutes), AuNR@SiO_2-d-CPP group (PTT by 808 nm 2 W laser irradiation for 5 minutes), and Ce6-AuNR@SiO_2-d-CPP group (PTT/PDT by 808 nm 2 W irradiation for 5 minutes and 650 nm 50 mW irradiation for 5 minutes). Data are presented as the mean±SD (n=6). Arrows indicate the drug-dosing time points. $P<0.05$; a, vs physiological saline; b, vs free Ce6; c, vs AuNR@SiO_2-d-CPP.

Abbreviations: AuNR, Au nanorod; Ce6, chlorin e6; Ce6-AuNR@SiO_2-d-CPP, chlorin gold nanorods; d-CPP, D-type cell penetrating peptide; PTT/PDT, photothermal/photodynamic therapy.

for treatment of breast cancer by PTT/PDT. Therefore, the present study could offer a new promising strategy to circumvent the dilemma in the clinical treatment of breast cancer.

Acknowledgments

This work was funded by the National Natural Science Foundation of China (grant nos. 81373343 and 81673367) and Innovation Team of Ministry of Education (no. BMU2017TD003).

Disclosure

The authors report no conflicts of interest in this work.

References

1. Siegel RL, Miller KD, Jemal A. Cancer statistics, 2016. *CA Cancer J Clin*. 2016;66(1):7–30.
2. Desantis C, Siegel R, Bandi P, Jemal A. Breast cancer statistics, 2011. *CA Cancer J Clin*. 2011;61(6):408–418.
3. Tanwar J, Das S, Fatima Z, Hameed S. Multidrug resistance: an emerging crisis. *Interdiscip Perspect Infect Dis*. 2014;2014(12):541340–541347.
4. Yu DD, Wu Y, Shen HY, et al. Exosomes in development, metastasis and drug resistance of breast cancer. *Cancer Sci*. 2015;106(8):959–964.
5. Cady B. Local therapy and survival in breast cancer. *N Engl J Med*. 2007;357(10):1051.
6. Soliman H. Immunotherapy strategies in the treatment of breast cancer. *Cancer Control*. 2013;20(1):17–21.
7. Bhana S, O'Connor R, Johnson J, Ziebarth JD, Henderson L, Huang X. Photosensitizer-loaded gold nanorods for near infrared photodynamic and photothermal cancer therapy. *J Colloid Interface Sci*. 2016;469:8–16.
8. Weissleder R, Ntziachristos V. Shedding light onto live molecular targets. *Nat Med*. 2003;9(1):123–128.
9. Weissleder R. A clearer vision for in vivo imaging. *Nat Biotechnol*. 2001;19(4):316–317.
10. Diaby V, Tawk R, Sanogo V, Xiao H, Montero AJ. A review of systematic reviews of the cost-effectiveness of hormone therapy, chemotherapy, and targeted therapy for breast cancer. *Breast Cancer Res Treat*. 2015;151(1):27–40.
11. Milletti F. Cell-penetrating peptides: classes, origin, and current landscape. *Drug Discov Today*. 2012;17(15–16):850–860.
12. Roveri M, Bernasconi M, Leroux J-C, Luciani P. Peptides for tumor-specific drug targeting: state of the art and beyond. *J Mater Chem B*. 2017;5(23):4348–4364.
13. Zhang X, Jin Y, Plummer MR, Pooyan S, Gunaseelan S, Sinko PJ. Endocytosis and membrane potential are required for HeLa cell uptake of R.I.-CKTat9, a retro-inverso Tat cell penetrating peptide. *Mol Pharm*. 2009;6(3):836–848.
14. Connor EE, Mwamuka J, Gole A, Murphy CJ, Wyatt MD. Gold nanoparticles are taken up by human cells but do not cause acute cytotoxicity. *Small*. 2005;1(3):325–327.
15. Zhang Z, Wang L, Wang J, et al. Mesoporous silica-coated gold nanorods as a light-mediated multifunctional theranostic platform for cancer treatment. *Adv Mater*. 2012;24(11):1418–1423.
16. Rana S, Bajaj A, Mout R, Rotello VM. Monolayer coated gold nanoparticles for delivery applications. *Adv Drug Deliv Rev*. 2012;64(2):200–216.
17. Nikoobakht B, El-Sayed MA. Preparation and growth mechanism of gold nanorods (NRs) using seed-mediated growth method. *Chem Mater*. 2003;15(10):1957–1962.
18. Gole A, Murphy CJ. Seed-mediated synthesis of gold nanorods: role of the size and nature of the seed. *Chem Mater*. 2004;16(19):3633–3640.
19. Stöber W, Fink A, Bohn E. Controlled growth of monodisperse silica spheres in the micron size range. *J Colloid Interface Sci*. 1968;26(1):62–69.
20. Bainor A, Chang L, McQuade TJ, Webb B, Gestwicki JE. Bicinchoninic acid (BCA) assay in low volume. *Anal Biochem*. 2011;410(2):310–312.
21. Copolovici DM, Langel K, Eriste E, Langel Ü. Cell-penetrating peptides: design, synthesis, and applications. *ACS Nano*. 2014;8(3):1972–1994.
22. Guo Z, Gu C, Fan X, et al. Fabrication of anti-human cardiac troponin i immunogold nanorods for sensing acute myocardial damage. *Nanoscale Res Lett*. 2009;4(12):1428–1433.
23. Thorén PE, Persson D, Isakson P, Goksör M, Önfelt A, Nordén B. Uptake of analogs of penetratin, Tat(48–60) and oligoarginine in live cells. *Biochem Biophys Res Commun*. 2003;307(1):100–107.
24. Rattanapinyopituk K, Shimada A, Morita T, et al. Demonstration of the clathrin- and caveolin-mediated endocytosis at the maternal-fetal barrier in mouse placenta after intravenous administration of gold nanoparticles. *J Vet Med Sci*. 2014;76(3):377–387.
25. Almeida PF, Pokorny A. Mechanisms of antimicrobial, cytolytic, and cell-penetrating peptides: from kinetics to thermodynamics. *Biochemistry*. 2009;48(34):8083–8093.
26. Li Y, Lei Y, Wagner E, et al. Potent retro-inverso D-peptide for simultaneous targeting of angiogenic blood vasculature and tumor cells. *Bioconjug Chem*. 2013;24(1):133–143.
27. Zhang X, Wan L, Pooyan S, et al. Quantitative assessment of the cell penetrating properties of RI-Tat-9: evidence for a cell type-specific barrier at the plasma membrane of epithelial cells. *Mol Pharm*. 2004;1(2):145–155.
28. Cherukuri P, Glazer ES, Curley SA. Targeted hyperthermia using metal nanoparticles. *Adv Drug Deliv Rev*. 2010;62(3):339–345.
29. Milleron RS, Bratton SB. "Heated" debates in apoptosis. *Cell Mol Life Sci*. 2007;64(18):2329–2333.
30. Castano AP, Mroz P, Hamblin MR. Photodynamic therapy and anti-tumour immunity. *Nat Rev Cancer*. 2006;6(7):535–545.
31. Hong EJ, Choi DG, Shim MS. Targeted and effective photodynamic therapy for cancer using functionalized nanomaterials. *Acta Pharm Sin B*. 2016;6(4):297–307.
32. Rajendran M. Quinones as photosensitizer for photodynamic therapy: ROS generation, mechanism and detection methods. *Photodiagnosis Photodyn Ther*. 2016;13:175–187.
33. de Groot DJ, Timmer T, Spierings DC, Le TK, de Jong S, de Vries EG. Indomethacin-induced activation of the death receptor-mediated apoptosis pathway circumvents acquired doxorubicin resistance in SCLC cells. *Br J Cancer*. 2005;92(8):1459–1466.
34. Zhang BF, Xing L, Cui PF, et al. Mitochondria apoptosis pathway synergistically activated by hierarchical targeted nanoparticles co-delivering siRNA and lonidamine. *Biomaterials*. 2015;61:178–189.
35. Bernardi P, Rasola A, Forte M, Lippe G. The mitochondrial permeability transition pore: channel formation by f-atp synthase, integration in signal transduction, and role in pathophysiology. *Physiol Rev*. 2015;95(4):1111–1155.
36. Park MH, Jo M, Won D, et al. Snake venom toxin from Vipera lebetina turanica induces apoptosis of colon cancer cells via upregulation of ros- and jnk-mediated death receptor expression. *BMC Cancer*. 2012;12(1):228.
37. Awasthi VD, Garcia D, Goins BA, Phillips WT. Circulation and biodistribution profiles of long-circulating PEG-liposomes of various sizes in rabbits. *Int J Pharm*. 2003;253(1–2):121–132.
38. Prabhakar U, Maeda H, Jain RK, et al. Challenges and key considerations of the enhanced permeability and retention effect for nanomedicine drug delivery in oncology. *Cancer Res*. 2013;73(8):2412–2417.
39. Li Y, Wen G, Wang D, et al. A complementary strategy for enhancement of nanoparticle intracellular uptake. *Pharm Res*. 2014;31(8):2054–2064.

Supplementary materials

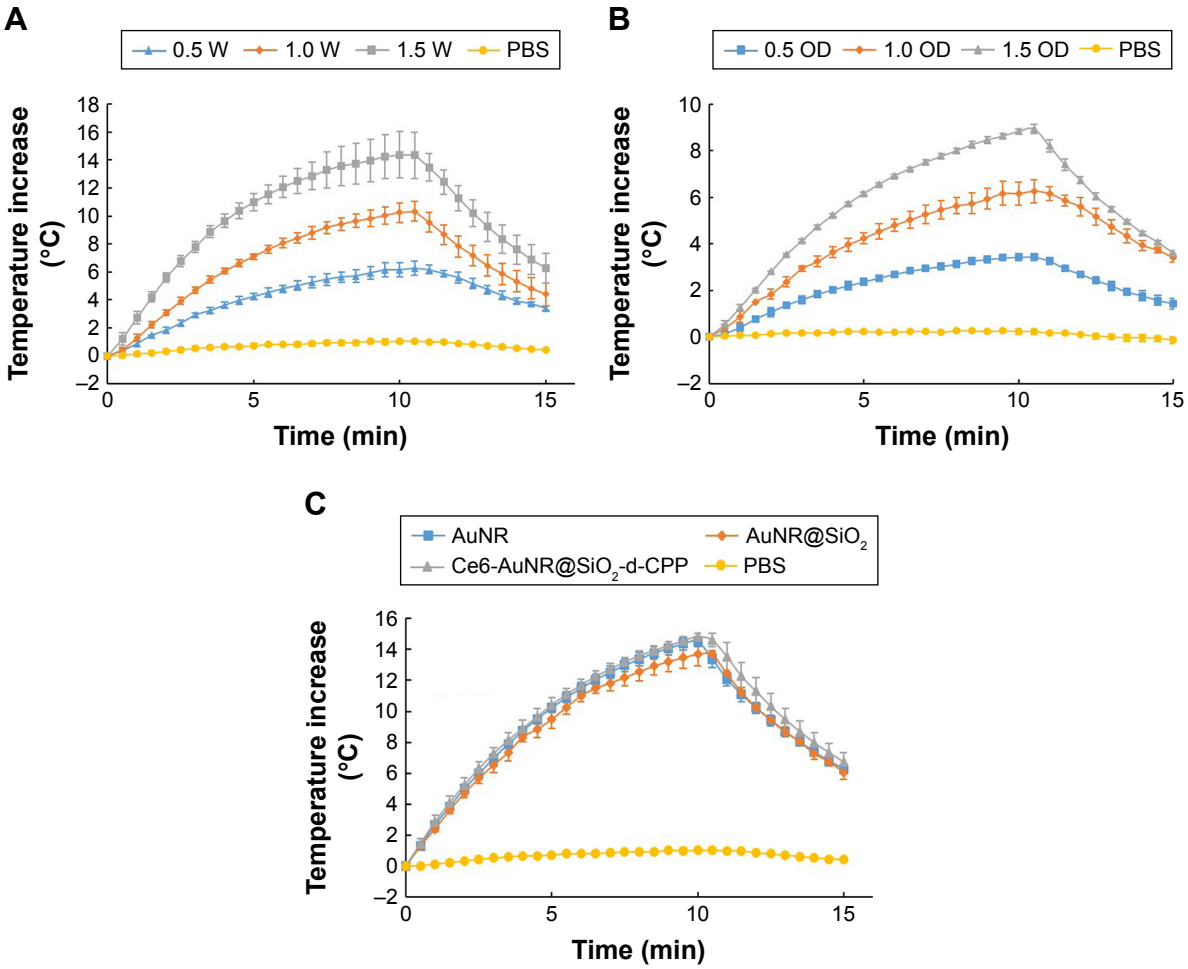

Figure S1 Photothermal effects of functional chlorin gold nanorods under the different treatment conditions.
Note: (**A**) Photothermal effects of functional chlorin gold nanorods under varying laser powers at 808 nm (AuNR solution fixed at 1 OD); (**B**) Photothermal effects of functional chlorin gold nanorods under varying AuNR concentrations (laser power fixed at 0.5 W); (**C**) Photothermal effects of functional chlorin gold nanorods under different kinds of AuNR formulations (808nm laser power fixed at 1.5 W). Data are presented as mean ± standard deviation (n=3).
Abbreviations: AuNR, Au nanorod; Ce6, chlorin e6; Ce6-AuNR@SiO_2-d-CPP, chlorin gold nanorods; d-CPP, D-type cell penetrating peptide.

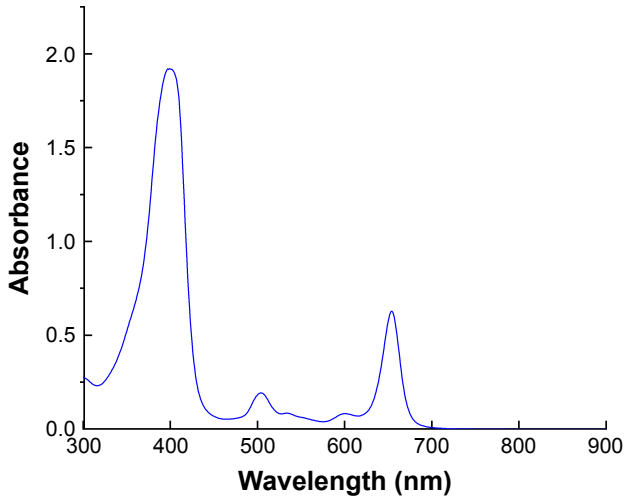

Figure S2 Vis-NIR spectrum of Ce6 solution (PBS 7.4).
Note: Ce6 has strong absorption peaks at 404, 503, and 667 nm, suggesting that the irradiation at 650 nm for PDT would not influence the irradiation at 808 nm for PTT (Figure S2), thus avoiding mutual interference of PTT and PDT during the experimental treatment.
Abbreviations: Ce6, chlorin e6; PTT/PDT, photothermal/photodynamic therapy; Vis-NIR, visible–near infrared.

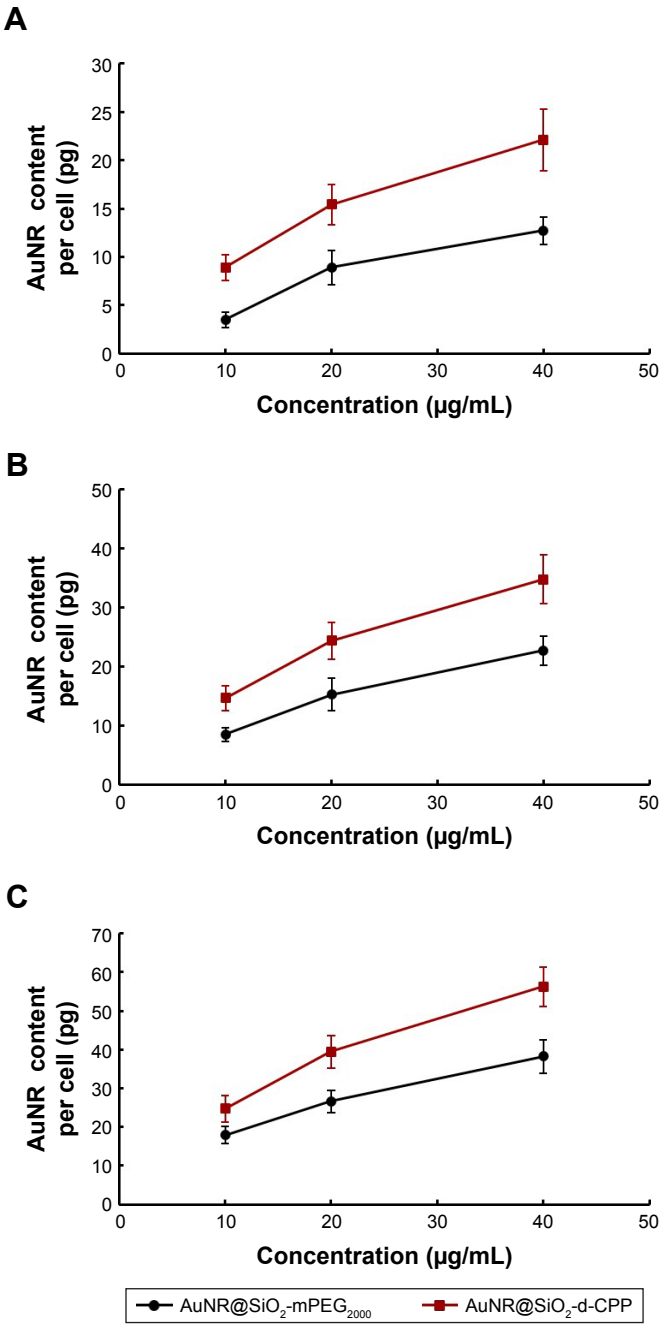

Figure S3 Uptake of AuNR@SiO$_2$-mPEG$_{2000}$ and AuNR@SiO$_2$-d-CPP by breast cancer cells.
Notes: The concentrations based on AuNR@SiO$_2$-mPEG$_{2000}$ were 10, 20, and 40 μg/mL, while the incubation times were (**A**) 3 hours, (**B**) 6 hours, and (**C**) 12 hours. Data are presented as the mean ± SD (n=3).
Abbreviations: AuNR, Au nanorod; Ce6, chlorin e6; Ce6-AuNR@SiO$_2$-d-CPP, chlorin gold nanorods; d-CPP, D-type cell penetrating peptide; PEG, polyethylene glycol.

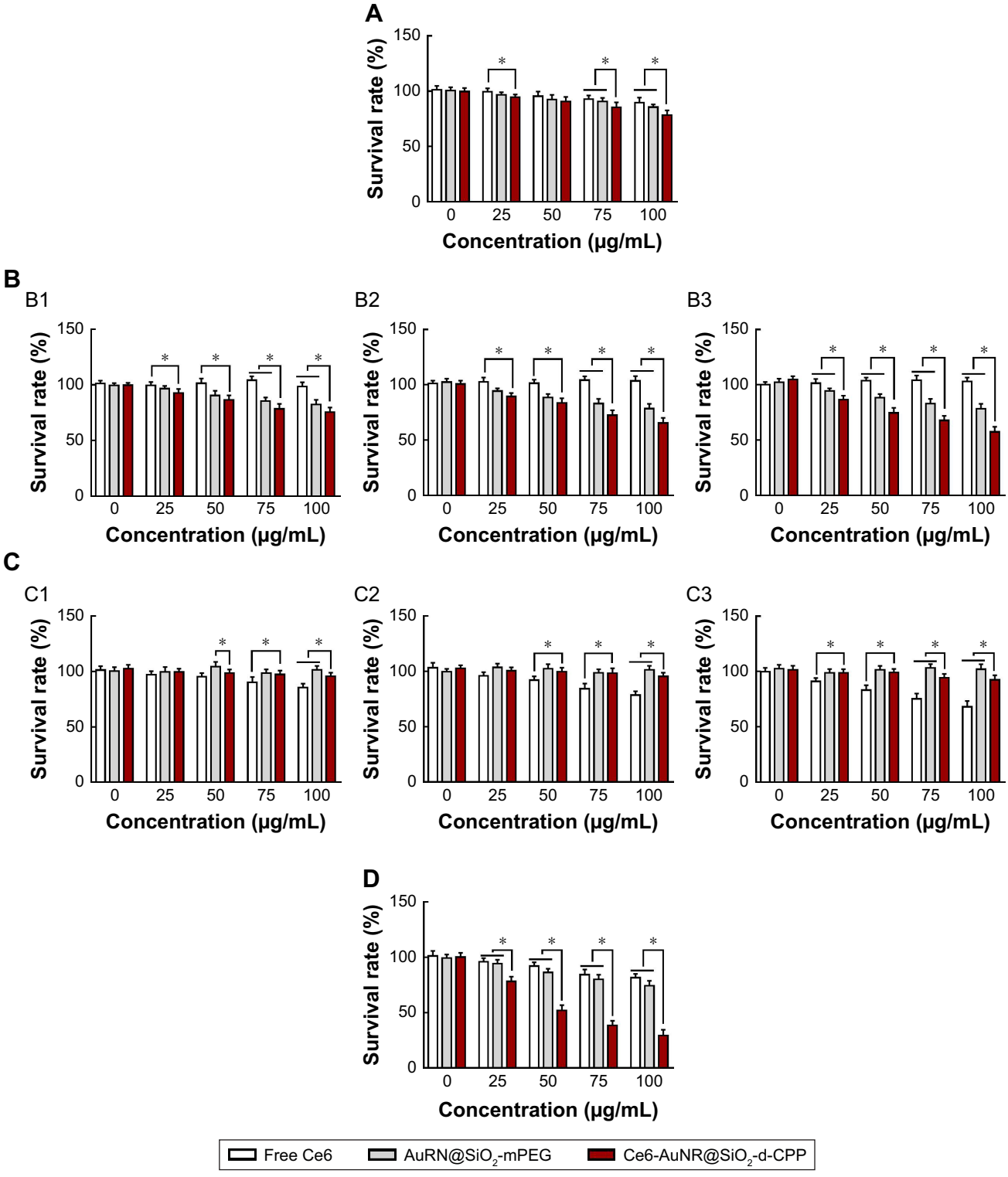

Figure S4 Cytotoxicity to breast cancer cells at varying concentrations of Ce6, AuNR@SiO_2-mPEG, and Ce6-AuNR@SiO_2-d-CPP in different mode.

Note: (**A**) Cytotoxicity in the dark; (**B**) photothermal effects after 3 minutes (B1), 5 minutes (B2), and 10 minutes (B3) 808 nm NIR irradiation; (**C**) photodynamical effects after 5 minutes (C1), 10 minutes (C2), and 15 minutes (C3) 650 nm NIR irradiation; (**D**) photothermal/photodynamic effects by combining 10 minutes 808 nm and 10 minutes 650 nm irradiation. Data are presented as the mean ± SD (n=3). *$P<0.05$, vs controls.

Abbreviations: AuNR, Au nanorod; Ce6, chlorin e6; Ce6-AuNR@SiO_2-d-CPP, chlorin gold nanorods; d-CPP, D-type cell penetrating peptide; NIR, near infrared; PEG, polyethylene glycol.